

Magnetically Torqued Neutrino-Dominated Accretion Flows for Gamma-ray Bursts

W. H. Lei¹, D. X. Wang^{1,2}, L. Zhang¹, Z. M. Gan¹, Y. C. Zou¹

School of Physics, Huazhong University of Science and Technology, Wuhan, 430074, China

and

Y. Xie³

School of Physics and Information Engineering, Shanxi Normal University, Linfen, 041004,
China

Received _____; accepted _____

¹School of Physics, Huazhong University of Science and Technology, Wuhan, 430074, China

²Send offprint requests to: D. X. Wang (dxwang@mail.hust.edu.cn)

³School of Physics and Information Engineering, Shanxi Normal University, Linfen, 041004, China

ABSTRACT

Recent observations and theoretical work on gamma-ray bursts (GRBs) favor the central engine model of a Kerr black hole (BH) surrounded by a magnetized neutrino-dominated accretion flow (NDAF). The magnetic coupling between the BH and disk through a large-scale closed magnetic field exerts a torque on the disk, and transports the rotational energy from the BH to the disk. We investigate the properties of the NDAF with this magnetic torque. For a rapid spinning BH, the magnetic torque transfers enormous rotational energy from BH into the inner disk. There are two consequences: (i) the luminosity of neutrino annihilation is greatly augmented; (ii) the disk becomes thermally and viscously unstable in the inner region, and behaves S-Shape of the surface density versus accretion rate. It turns out that magnetically torqued NDAF can be invoked to interpret the variability of gamma-ray luminosity. In addition, we discuss the possibility of restarting the central engine to produce the X-ray flares with required energy.

Subject headings: accretion, accretion disk– black hole physics – magnetic fields – gamma rays: bursts – neutrinos

1. INTRODUCTION

The nature of the central engine of gamma-ray bursts (GRBs) remains unclear. Currently favored models invoke a binary merger or a collapse of compact objects. These models lead to the formation of a transient hot and dense accretion torus/disk around a black hole (BH) of a few solar masses.

The typical mass accretion rates in GRB models are extremely high, of the order of a fraction of solar mass up to a few solar masses per second. Under such conditions, the disk becomes dense and hot enough in the inner regions to cool via neutrino losses. For this reason, Popham, Woosley & Fryer (1999, hereafter PWF99) named these disk neutrino-dominated accretion flows (NDAF). Energy extraction from the BH-accretion disk for powering GRB is also possible, such as by Blandford-Znajek (BZ) process (see Lee et al. 2000 for a review of this model), and Blandford-Payne (BP) process and Parker instabilities in the disk (Narayan et al. 1992; Meszaros & Rees 1997).

NDAF has been extensively discussed by many authors, e.g., PWF99, Narayan, Piran & Kumar (2001, hereafter NPK01), Kohri & Mineshige (2002), Di Matteo, Perna & Narayan (2002, hereafter DPN), Chen & Beloborodov (2006), Janiuk et al. (2004, 2007) and Gu, Liu & Lu (2006, hereafter GLL06). However, due to its low energy conversion efficiencies and the effects of neutrino opacity, the power produced by neutrino-antineutrino annihilation can hardly match those of the energetic short-hard GRBs (e.g. GRB080913) and X-ray flares. Recently, some authors (e.g., DPN02, Fan et al. 2005, Shibata et al. 2006 and 2007 and Perez-Ramirez et al. 2008) suggested that the MHD process should be considered in the disk model. Moreover, as shown in Shibata et al. (2006, 2007), the magnetic braking and magneto-rotational instability (MRI, Balbus & Hawley 1991) in the disk play a role in angular momentum transporting, which causes turbulent motion, resultant shock heating, and mass accretion onto the BH. On the other hand, researches showed that the magnetic

fields can be magnified up to $10^{15} \sim 10^{16}$ G by virtue of MRI or dynamo process (Pudritz & Fahlman 1982 and references therein) in hyperaccretion disk. These considerations stimulate us to discuss the magnetized NDAF.

Based on the work of NPK01 and DPN02, Xie et al. (2007) discussed the BZ and BP processes in NDAF. They found that the jet of GRB may be magnetically-dominated, which is also obtained by MHD simulations of Mizuno et al.(2004).

Recently, the magnetic coupling (MC) between the central spinning BH and their surrounding accretion disk has been paid much attention (e.g. Blandford 1999; van Putten 1999; Li & Paczynski 2000; Li 2002; Wang et al. 2002). As a variant of the BZ process, the MC process exerts a torque on the disk, and transports the rotational energy from the BH to the disk. The effects of MC torque has been discussed in some disk models, for example, Lai (1998) and Lee (1999) in a neutron star with slim disk, Li (2002), Wang et al. (2002, 2003), Kluzniak and Rappaport (2007) in a compact object with thin disk, Ye et al. (2007) and Ma et al. (2007) in a BH with advection-dominated accretion flow (ADAF). It is found, the disk properties are greatly changed and its luminosity is augmented significantly due to the rotational energy of BH extracted in the MC process. Therefore, it is attractive for us to investigate the effects of MC torque on NDAF. To highlight the effects of MC torque, we ignore other MHD process, such as BZ and BP mechanism, and we refer to this model as MCNDAF.

This paper is organized as follows. In Sect. 2 we describe the MCNDAF model, which is a relativistic steady state thin disk. The effects of MHD stress are described by the dimensionless parameter α . The main equations are based on DPN02 and NPK01. Recently, GLL06, Chen & Beloborodov (2006) and Shibata et al. (2006, 2007) argued that the general relativistic (GR) effects are important for NDAF, so we introduce GR correction factors to the equations. The MC torque appears in the angular momentum equation.

We solve the set of equations for the solutions in MCNDAF in Sect. 3, and compute the neutrino and neutrino annihilation luminosities. Following GLL06, we include the neutrino radiation from the optically thick region in the computation for the neutrino luminosity. To show the effects of MC torque, we compare it with previous results. In Sect. 4 we discuss the stability of the accretion flow. We also discuss the physical origin of the instabilities in MCNDAF. Finally, we summarize our results and discuss some related issues in Sect. 5.

2. NEUTRINO-DOMINATED ACCRETION FLOWS WITH MC EFFECTS

Considering that central BHs are rapidly rotating in most candidate GRB engines, we discuss a model of a steady state disk around a Kerr BH, in which neutrino loss and transfer are taken into account. Our model is presented in the context given by DPN02, and the GR corrections are adopted from Riffert & Herold (1995).

As mentioned by DPN02 and PWF99, although in GRB central engines the accretion rate may vary, it is expected to vary significantly only in the outer disk. Hence it seems reasonable to study the main properties in the inner neutrino-cooled disk by assuming a constant accretion rate.

Because the gas cools efficiently, we are entitled to discuss the MCNDAF model in the context of a thin disk (Shakura & Sunyaev 1973). The accuracy of the thin-disk approximation is not perfect at large radii, where the disk is thick. Fortunately, the details of the outer region have little effect on the solution for the neutrino-cooled disk (Chen & Beloborodov 2006).

The MCNDAF model is a relativistic steady thin disk, and the large-scale magnetic field contributing to the MC process and the small-scale tangled magnetic field related to the viscosity are included. We assume that these two kinds of fields work independently,

and the large-scale magnetic field remains constant at the BH horizon. Following Blandford (1976) we assume that the magnetic field B_z on the disk varies as $B_z \propto \xi^{-n}$, where $\xi \equiv r/r_{ms}$ is the disk radius in terms of the marginally stable orbit r_{ms} (Novikov & Thorne 1973), and n is the power law index indicating the degree of concentration of the magnetic field in the central region of the disk.

Based on equipartition relation the magnetic field at the horizon is related to the mass density at the inner disk as follows (McKinney 2005),

$$\frac{B_H^2}{8\pi} = \rho_{0,disk} c^2, \quad (1)$$

where $\rho_{0,disk} \equiv \dot{M} t_g / r_g^3$, $t_g = GM/c^3$ and $r_g = GM/c^2$.

The MC torque is derived in Wang et al. (2002) based on an equivalent circuit given by Macdonald & Thorne (1982) as follows,

$$T_{MC}/T_0 = 4a_*(1+q) \int_0^{\pi/2} \frac{(1-\beta) \sin^3 \theta d\theta}{2 - (1-q) \sin^2 \theta} \quad (2)$$

where $T_0 \approx 3.26 \times 10^{45} (\frac{B_H}{10^{15} G})^2 (\frac{M}{M_\odot})^3 g \cdot cm^2 \cdot s^{-2}$, $a_* \equiv Jc/(GM^2)$ is the dimensionless BH spin parameter defined by the BH mass M and angular momentum J , $q = \sqrt{1-a_*^2}$ and $\beta \equiv \Omega_D/\Omega_H$ is the ratio of the angular velocity of the disk $\Omega_D = ((r^3/GM)^{1/2} + a_* GM/c^3)^{-1}$ to that of the horizon $\Omega_H = a_* c^3/[2GM(1+q)]$.

The mapping relation between the angular coordinate θ on the horizon and the radial coordinate ξ on the disk is derived based on the conservation of magnetic flux as follows (Wang et al. 2003),

$$\cos \theta = \int_1^\xi \Theta(a_*; \xi, n) d\xi \quad (3)$$

where $\xi = (r/r_{ms})^{1/2}$,

$$\Theta(a_*; \xi, n) = \frac{\xi^{1-n} \chi_{ms}^2 \sqrt{1 + a_*^2 \chi_{ms}^{-4} \xi^{-2} + 2a_*^2 \chi_{ms}^{-6} \xi^{-3}}}{2\sqrt{(1 + a_*^2 \chi_{ms}^{-4} + 2a_*^2 \chi_{ms}^{-6})(1 - 2\chi_{ms}^{-2} \xi^{-1} + a_*^2 \chi_{ms}^{-4} \xi^{-2})}}. \quad (4)$$

where $\chi_{ms} = (r_{ms}/r_g)^{1/2}$.

A number of works (PWF99; Chen & Beloborodov, 2006) used accurate equations of relativistic hydrodynamics in Kerr spacetime to study NDAF. GLL06 found that the GR effect must be taken into account for the power of GRB.

The relativistic correction factors for a thin accretion disk around a Kerr BH have been given by Riffert & Herold (1995),

$$A = 1 - \frac{2GM}{c^2 r} + \left(\frac{GMa_*}{c^2 r}\right)^2, \quad (5)$$

$$B = 1 - \frac{3GM}{c^2 r} + 2a_* \left(\frac{GM}{c^2 r}\right)^{3/2}, \quad (6)$$

$$C = 1 - 4a_* \left(\frac{GM}{c^2 r}\right)^{3/2} + 3\left(\frac{GMa_*}{c^2 r}\right)^2, \quad (7)$$

$$D = \int_{r_{ms}}^r \frac{\frac{x^2 c^4}{8G^2} - \frac{3xMc^2}{4G} + \sqrt{\frac{a_*^2 M^3 c^2 x}{G} - \frac{3a_*^2 M^2}{8}}}{\frac{\sqrt{rx}}{4} \left(\frac{x^2 c^4}{G^2} - \frac{3xMc^2}{G} + 2\sqrt{\frac{a_*^2 M^3 c^2 x}{G}}\right)} dx. \quad (8)$$

The equation of the conservation of mass remains valid, while hydrostatic equilibrium in the vertical direction leads to a corrected expression for the half thickness of the disk (Riffert & Herold 1995; Reynoso, Romero & Sampayo 2006):

$$H \simeq \sqrt{\frac{Pr^3}{\rho GM}} \sqrt{\frac{B}{C}}. \quad (9)$$

The viscous shear $t_{r\varphi}$ is corrected by

$$t_{r\varphi} = -\alpha P \sqrt{\frac{A}{BC}}. \quad (10)$$

The basic equations of MCNDAF are given as follows.

1. The continuity equation:

$$\dot{M} = -2\pi r v_r \Sigma. \quad (11)$$

2. The total pressure consists of five terms, radiation pressure, gas pressure, degeneracy pressure, neutrino pressure and magnetic pressure:

$$P = \frac{11}{12} a T^4 + \frac{\rho k T}{m_p} \left(\frac{1 + 3X_{nuc}}{4} \right) + \frac{2\pi \hbar c}{3} \left(\frac{3}{8\pi m_p} \right)^{4/3} \left(\frac{\rho}{\mu_e} \right)^{4/3} + \frac{u_\nu}{3} + P_{mag}. \quad (12)$$

where $P_{mag} = \beta_t P$ is the magnetic pressure contributed by the tangled magnetic field in the disk, and β_t is the ratio of the magnetic pressure to the total pressure. u_ν is the neutrino energy density defined as (Popham & Narayan 1995)

$$u_\nu = (7/8) a T^4 \sum \frac{\tau_{\nu_i}/2 + 1/\sqrt{3}}{\tau_{\nu_i}/2 + 1/\sqrt{3} + 1/(3\tau_{a,\nu_i})} \quad (13)$$

In equation (13) $\tau_{\nu_i} = \tau_{a,\nu_i} + \tau_{s,\nu_i}$ is the sum of absorptive and scattering optical depths calculated for each neutrino flavor (ν_e, ν_μ, ν_τ). The absorptive optical depths for the three neutrino flavors are (Kohri et al. 2005)

$$\tau_{a,\nu_e} \simeq 2.5 \times 10^{-7} T_{11}^5 H + 4.5 \times 10^{-7} T_{11}^2 X_{nuc} \rho_{10} H, \quad (14)$$

$$\tau_{a,\nu_\mu} = \tau_{a,\nu_\tau} \simeq 2.5 \times 10^{-7} T_{11}^5 H, \quad (15)$$

where X_{nuc} is the mass fraction of free nucleons approximately given by (e.g., PWF99; Qian & Woosley 1996),

$$X_{nuc} \simeq 34.8 \rho_{10}^{-3/4} T_{11}^{9/8} \exp(-0.61/T_{11}). \quad (16)$$

The total scattering optical depth is given by DPN02 as

$$\tau_{s,\nu_i} \simeq 2.7 \times 10^{-7} T_{11}^2 \rho_{10} H. \quad (17)$$

3. Combining the conservation of the angular momentum with equation (11), we have

$$\frac{d}{dr}(\dot{M}l) + 4\pi r H_{MC} = \frac{d}{dr}g = -\frac{d}{dr}(4\pi r^2 t_{r\varphi} H), \quad (18)$$

where l is the specific angular momentum of the accreting gas. The flux of angular momentum transferred magnetically from the BH to the disk, H_{MC} , is related to the MC torque T_{MC} by

$$T_{MC} = 4\pi \int_{r_{ms}}^r H_{MC} r dr. \quad (19)$$

Vanishing of $t_{r\varphi}$ (or g) at r_{ms} leads to

$$\dot{M}r^2\sqrt{\frac{GM}{r^3}}\frac{D}{A} + T_{MC} = g = -4\pi r^2 t_{r\varphi} H = 4\pi r^2 H \alpha P \sqrt{\frac{A}{BC}} \quad (20)$$

4. The equation for the energy balance is

$$Q^+ = Q^- \quad (21)$$

where $Q^+ = Q_{vis}$ represents the viscous dissipation, and $Q^- = Q_\nu + Q_{photo} + Q_{adv}$ is the total cooling rate due to neutrino losses Q_ν , photodisintegration Q_{photo} and advection Q_{adv} . We employ a bridging formula for calculating Q_ν , which is valid in both the optically thin and thick cases. The expressions for Q_ν , Q_{photo} and Q_{adv} are (DPN02; GLL06)

$$Q_\nu = \sum \frac{(7/8\sigma T^4)}{(3/4)(\tau_{\nu_i}/2 + 1/\sqrt{3} + 1/(3\tau_{a,\nu_i}))}, \quad (22)$$

$$Q_{photo} = 10^{29} \rho_{10} v_r \frac{dX_{nuc}}{dr} H \text{ erg} \cdot \text{cm}^{-2} \text{s}^{-1}, \quad (23)$$

$$Q_{adv} \simeq v_r \frac{H}{r} \left(\frac{11}{3} aT^4 + \frac{3}{2} \frac{\rho kT}{m_p} \frac{1 + X_{nuc}}{4} + \frac{4u_\nu}{3} \right), \quad (24)$$

where $4u_\nu/3$ is the entropy density of neutrinos. Note that the cooling function given by the bridging formula reduces to the optically thin expression for small optical depths (as adopted in PWF99) but differs significantly from the latter at optical depths ~ 1 .

By considering the MC effects, the heating rate Q_{vis} is expressed as

$$Q_{vis} = -\frac{g\Omega'_D}{4\pi r} = \frac{3GM\dot{M}}{8\pi r^3} \frac{D}{B} - \frac{T_{MC}\Omega'_D}{4\pi r}, \quad (25)$$

where the second term is the MC contribution.

As we can see from equation (20), the magnetic torque may deposit angular momentum in the inner disk, and this extra angular momentum must be transported outwards by the viscous torque in the disk, resulting in energy dissipation and increasing the disk luminosity based on equation (25).

Defining $Q_G = 3GM\dot{M}D/(8\pi r^3 B)$ and $Q_{MC} = -T_{MC}\Omega'_D/(4\pi r)$ as the contributions due to the gravitational release and the MC process, respectively, we have the ratio $\eta \equiv Q_{MC}/Q_G$ versus the disk radius $R \equiv r/r_g$ as shown in Figure 1.

From Figure 1 we find that Q_{MC} is much greater than Q_G in the inner disk, where the neutrino cooling dominates. The ratio η is very sensitive to the value of a_* and n , it increases monotonically with the increasing a_* and n . This implies that the MC effects are more important for the greater a_* and n . For simplicity, we choose $a_* = 0.9$ and $n=3$ in the calculations, and discuss the influence of their values in Sect. 5.

We solve numerically equations (12), (20) and (21) to find the disk temperature T and density ρ versus the disk radius with the given a_* , n and \dot{m} (where \dot{m} is the accretion rate in units of $M_\odot s^{-1}$). We take $X_{nuc} = 1$ for the fully photodisintegrated nuclear, which is appropriate in the inner disk. In the calculation, we do not include the cooling term arising from the photodisintegration, because it is much less than the neutrino cooling rate in the inner disk (Janiuk et al. 2004). Furthermore, $\alpha = 0.1$, $M = 7M_\odot$ and $\beta_t = 0.1$ are adopted in calculations.

3. EFFECTS OF THE MC TORQUE ON NEUTRINO ANNIHILATION LUMINOSITY

As discussed in Sect. 2, the MC process applies a strong torque on the disk, resulting in huge viscous dissipation. This would lead to a more powerful neutrino radiation, and

neutrino annihilation luminosity. Here, we will show the effects of MC torque on the neutrino annihilation luminosity.

To show this, we compare the results of MCNDAF with the NDAF model without MC (hereafter NDAF refers to the model without MC). GLL06 pointed out that the GR effects and the neutrino radiation from the optically thick region are important for the NDAF luminosity. Therefore we include these two effects in our calculations for both MCNDAF and NDAF.

The neutrino luminosity from the accretion flow is

$$L_\nu = 4\pi \int_{r_{ms}}^{r_{out}} Q_\nu r dr. \quad (26)$$

We are interested primarily in the properties of the inner accretion flow, where neutrino processes are important. As argued in PWF99, NPK01 and DPN02, the flows are fully advection-dominated for $r > 100r_g$, since neutrino cooling is not important and photons are completely trapped. Thus we concentrate the discussion in the region from r_{ms} to $r_{max} = 100r_g$.

Our method for calculating neutrino annihilation is similar to PWF99 and Rosswog et al. (2003). The disk is modeled as a grid of cells in the equatorial plane. A cell k has its neutrino mean energy $\epsilon_{\nu_i}^k$ and luminosity $l_{\nu_i}^k$, and the height above (or below) the disk is d_k . The angle at which neutrinos from cell k encounter antineutrinos from another cell k' at that point is denoted as $\theta_{kk'}$. Then the neutrino annihilation luminosity at that point is given by the summation over all pairs of cells,

$$l_{\nu\bar{\nu}} = A_1 \sum_k \frac{l_{\nu_i}^k}{d_k^2} \sum_{k'} \frac{l_{\bar{\nu}_i}^{k'}}{d_{k'}^2} (\epsilon_{\nu_i}^k + \epsilon_{\bar{\nu}_i}^{k'}) (1 - \cos\theta_{kk'})^2 + A_2 \sum_k \frac{l_{\nu_i}^k}{d_k^2} \sum_{k'} \frac{l_{\bar{\nu}_i}^{k'}}{d_{k'}^2} \frac{\epsilon_{\nu_i}^k + \epsilon_{\bar{\nu}_i}^{k'}}{\epsilon_{\nu_i}^k \epsilon_{\bar{\nu}_i}^{k'}} (1 - \cos\theta_{kk'}) \quad (27)$$

where $A_1 \approx 1.7 \times 10^{-44} \text{cm} \cdot \text{ergs}^{-2} \cdot \text{s}^{-1}$ and $A_2 \approx 1.6 \times 10^{-56} \text{cm} \cdot \text{ergs}^{-2} \cdot \text{s}^{-1}$.

The total neutrino annihilation luminosity is obtained by integrating over the whole space outside the BH and the disk,

$$L_{\nu\bar{\nu}} = 4\pi \iint l_{\nu\bar{\nu}} r dr dz \quad (28)$$

As shown in Figure 2, the variations of L_ν and $L_{\nu\bar{\nu}}$ versus \dot{m} for MCNDAF are indicated by the thin and thick solid lines, respectively, while those for NDAF are marked by the dotted and dashed lines, respectively. It is found that L_ν and $L_{\nu\bar{\nu}}$ are greatly strengthened in MCNDAF. This means the spin energy acts as a powerful source for NDAF.

According to our calculations for MCNDAF $L_{\nu\bar{\nu}}$ varies from $3.7 \times 10^{49} \text{ergs} \cdot \text{s}^{-1}$ to $1.4 \times 10^{54} \text{ergs} \cdot \text{s}^{-1}$ for $0.01 < \dot{m} < 10$. We find that $L_{\nu\bar{\nu}}$ nearly stays constant around $\sim 10^{54} \text{ergs} \cdot \text{s}^{-1}$ for the accretion rate above $\dot{m} \sim 0.5$. This implies that the effect of neutrino optical depth becomes important. Our results for NDAF are in good agreement with those given by PWF99 and GLL06, but larger than those in DPN02. This is because the GR effects are taken into account in this paper as well as in PWF99 and GLL06.

4. STABILITY ANALYSIS: THERMAL-VISCOUS INSTABILITY

DPN02 discussed the thermal, viscous and gravitational stability properties of NDAF solutions. They found that NDAF is stable in most cases. But this result is not consistent with the variability in GRB lightcurve. To explain the X-ray flares, it is need that after the prompt gamma-ray emission has ceased, the central engine can be restarted (Fan & Wei 2005; Zhang et al. 2006). Based on this scenario, Perna et al. (2006) suggested that the X-ray flares could be produced by accretion of matter after the breaking of the disk due to the setting up of various instabilities either gravitational or viscous. Therefore, it is

attractive for us to examine whether MCNDAF solution is stable.

The condition for viscous stability is given by

$$\frac{d\dot{M}}{d\Sigma} > 0, \quad (29)$$

The stability curves for several radii in the disk are shown in Figure 3.

From Figure 3, we find the $\dot{m} - \Sigma$ curves show S-Shape, in which the branch of solutions with negative slope is viscously unstable. It is shown that the viscous instability occurs at larger radius for larger accretion rate. However, we find this unstable can only occur at $\dot{m} > 0.086$, see Figure 5.

It is clearly shown in Figure 3 that the disk is unstable at $\dot{m} = 0.5$ for $R = 3$, $\dot{m} = 2$ for $R = 10$, and $\dot{m} = 10$ for $R = 20$. To understand this S-Shape we draw Figure 4.

Inspecting Figures 3 and 4, we find the viscous instability occurs when the disk is neutrino cooling and radiation pressure dominated. For $\dot{m} < 0.086$, the MC torque will become very small, and the disk is optically thin to neutrinos. As discussed in NPK01, an optically thin NDAF is viscously stable for all pressure cases. Therefore, we will find no viscous instability when $\dot{m} < 0.086$. If the accretion rate beyond $0.086M_{\odot}s^{-1}$, the MC torque transport enormous energy into the inner disk, and make the inner disk optically thick to neutrinos. In this time, we have $\dot{m} \propto \Sigma^{-1}$ for neutrino cooling and radiation pressure dominated case, and the disk will be viscously unstable. If gas pressure dominates, we have $\dot{m} \propto \Sigma$ and $\dot{m} \propto \Sigma^3$ for optically thin and thick NDAF, respectively. In the region where advection dominated, the disk is viscous stable, which is the well-known property of slim disk.

From the above analysis, we conclude that the appearance of the viscous instability is due to the MC torque. First, the MC torque results in an optically thick neutrino-cooling

dominated flow in the inner disk part for high accretion rates. Second, the high opacity will drop the neutrino-cooling rate, and leave a hot and thick disk. In this region, the gas pressure drops and radiation pressure becomes important. We checked that the unstable solutions appear for black hole spin $a_* > 0.35$ and magnetic pressure $\beta_t < 0.8$.

The disk is thermally unstable if $(d \ln Q^+ / d \ln T)|_\Sigma > (d \ln Q^- / d \ln T)|_\Sigma$. Then any small increase (decrease) in temperature leads to heating rate which is more (less) than the cooling rate, and as a consequence a further increase (decrease) of the temperature. For an optically thick NDAF in which neutrino cooling and radiation pressure dominates, we have $Q^+ \propto T^8 / \Sigma$ and $Q^- \propto T^4$. Therefore, the disk is also thermally unstable at the negative slope of the S-Shape $\dot{m} - \Sigma$ curves shown in Figure 3.

It is noticed that Janiuk et al. (2007) obtain the viscous instability occurring at $\dot{m} > 10$ without the S-Shape curves, which is caused by the behavior distribution for X_{nuc} and photodisintegration term. However, in MCNDAF, the photodisintegration term is not included and $X_{nuc} = 1$ is assumed for simplicity. Therefore, we infer that the S-Shape curves in MCNDAF arise from the MC effects.

Finally, we check the gravitational stability condition, for which the Toomre parameter Q_T should be larger than unity. For Keplerian disk, Q_T is given by $Q_T = c_s \kappa / (\pi G \Sigma) = \Omega_D^2 / (\pi G \rho)$. Q_T decrease with increasing r so that the flow is most unstable on the outside.

5. SUMMARY AND DISCUSSION

In this paper we investigate some properties in MCNDAF. The angular momentum deposited in the disk by the magnetic torque exerted by the BH leads to a substantial additional dissipation of energy in the disk, which is greater than that expected from

gravitational release alone. Therefore, we obtain a series of MCNDAF solutions being different significantly from NDAF.

The main results are summarized as follows.

1. The neutrino annihilation luminosity in MCNDAF varies from $3.7 \times 10^{49} \text{ergs} \cdot \text{s}^{-1}$ to $1.4 \times 10^{54} \text{ergs} \cdot \text{s}^{-1}$ for $0.01 < \dot{m} < 10$, while for NDAF the value range is from $1.2 \times 10^{45} \text{ergs} \cdot \text{s}^{-1}$ to $2.6 \times 10^{53} \text{ergs} \cdot \text{s}^{-1}$, i.e., it is greatly improved by the MC torque.

Recently, observations show that half of the Swift bursts exhibit X-ray flares. Fan et al. (2005) pointed out that the energy from NDAF cannot match the X-ray flares detected in GRB 050724 of ~ 100 s, which is also the time scale of the central engine. The time averaged isotropic luminosity of the X-ray flare component is $L_X \sim 10^{48} \text{ergs} \cdot \text{s}^{-1}$. If we assume that the total mass available for accretion is $\sim 1M_\odot$ (a typical value for the compact object merger scenarios and massive star collapse scenario), and that most of the mass is accreted during the X-ray flare phase, the time averaged accretion rate is about $0.01M_\odot \text{s}^{-1}$. At this accretion rate, the jet luminosity powered by neutrino annihilation is $L_{\nu\bar{\nu}} \sim 10^{45} \text{ergs} \cdot \text{s}^{-1}$ for NDAF without MC torque, and it is insufficient to power the X-ray flares. But the power produce by MCNDAF can satisfy this requirement.

Very recently, the new observation of the highest redshift ($z=6.7$) swift source GRB080913 puts a very strong constraint on the central engine (Perez-Ramirez et al. 2008). The duration of this short burst is $T_{90} = 8\text{s}$, and the isotropic energy required is $E_{iso} \approx 7 \times 10^{52} \text{ergs}$. If the central engine is NDAF without MC torque, the jet collimation factor obeys $f_\Omega < 7 \times 10^{-4}$, i.e., the jet should be strongly collimated. If invoke the MC torque in NDAF, the observed energy can be easily satisfied.

2. The disk becomes thermally and viscously unstable in its inner region for $\dot{m} > 0.086$. It is very interesting for us to obtain the $\dot{m} - \Sigma$ curves behaving S-Shape, which may

produce a limit-cycle activity. The disk is rather thick in the inner region, and therefore the thermal and viscous timescales are close to each other. The timescale for the unstable can be estimated by the viscous timescale, $t_{vis} = [1/(\alpha\Omega)](r/H)^2$, which is about 10ms at the inner disk. Following the discussions in Janiuk et al. (2007), these instabilities will lead to a variable energy output on millisecond timescales, which may correspond to the variability in the gamma-ray luminosity. The irregularity in the overall outflow can also help produce internal shocks. On the other hand, the thermal-viscous instability may be accompanied by the disk breaking, which can lead to the several episodic accretion events and explain the long-time activity accounting for the X-ray flares.

Therefore, the MCNDAF can easily power both GRBs and its X-ray flares, naturally interpret the variability in the gamma-ray luminosity, and explain the production of X-ray flares. However, there are several issues should be addressed.

First, in all of the MCNDAF solutions, we assume $n=3$ and a large BH spin $a_* = 0.9$ but does not give any reason. From Figure 1 we find the MC contribution is sensitive to a_* and n . Thus for very small BH spin and value of n , the MC effects may be ignored, and the solutions return to NDAF solutions. Considering that the BH is spun-down in the MC process, while it is spun-up in the accretion process. The two processes with opposite effects result in a state with an equilibrium spin a_*^{eq} . Calculation shows that a_*^{eq} is greater than 0.85 for $n > 3$. This result implies that the MC effects are dominant in the whole duration of GRB, for which a fast-spinning BH is the central engine.

Secondly, we made many simplifications in the MCNDAF model, such as we omit the photodisintegration term in the cooling rates, we assume the disk is thin, and a very simple magnetic configuration, and so on. Recently, Liu et al. (2007) took into account more realistic microphysics. Chen & Beloborodov (2006) worked out the NDAF solution under full Kerr metric. It is necessary to combine these effects with the MC process and work out

a more detailed model in the future.

Finally, our MCNDAF is steady. Recently, Janiuk et al. (2004, 2007) computed the time evolution of NDAF that proceeds during the burst. It is very interesting to investigate a time-dependent MCNDAF.

Recently, Zhang & Dai (2007) proposed a hyperaccretion disk around a neutron star. They found, compared with a BH disk, the hyperaccretion disk around a neutron star can be cooled more efficiently and produce a much higher neutrino luminosity. As discussed by Kluzniak & Rappaport (2007), the magnetic dipole of the neutron star can also torque the disk. Therefore, it is also attractive to consider the effects of the magnetic torque in the context of hyperaccretion disk around a neutron star.

We thank T. Liu for helpful discussions, and also thank the anonymous referee for his/her valuable comments and constructive suggestions”. This work is supported by National Natural Science Foundation of China under Grants 10873005, 10847127 and 10703002, the Research Fund for the Doctoral Program of Higher Education under grant 200804870050 and National Basic Research Program of China under Grant No. 2009CB824800.

REFERENCES

- Balbus S. A., & Hawley J. F., 1991, *ApJ*, 376, 214
- Blandford, R. D. 1976, *MNRAS*, 176, 465
- Blandford, R. D. 1999, in *ASP Conf. Ser. 160, Astrophysical Discs: An EC Summer School*, ed. J. A. Sellwood & J. Goodman (San Francisco: ASP), 265
- Blandford, R. D., & Payne, D. G. 1982, *MNRAS*, 199, 883
- Blandford, R. D., & Znajek, R. L. 1977, *MNRAS*, 179, 433
- Chen, W. X., & Beloborodov, A. M. 2007, *ApJ*, 657, 383
- Di Matteo, T., Perna, R., & Narayan, R. 2002, *ApJ*, 579, 706 (DPN02)
- Fan Y. Z., & Wei D. M., 2005, *MNRAS*, 364, L42
- Fan, Y. Z., Zhang, B. & Proga, D. 2005, *ApJ*, 635, L129
- Gu, W. M., Liu, T., & Lu, J. F., 2006, *ApJ*, 643, L87 (GLL06)
- Janiuk, A., Perna, R., Di Matteo, T., & Czerny, B. 2004, *MNRAS*, 355, 950
- Janiuk, A., Yuan, Y., Perna, R., & Di Matteo, T. 2007, *ApJ*, 664, 1011
- Kluzniak, W., & Rappaport, S. 2007, *ApJ*, 671, 1990
- Kohri, K., & Mineshige, S. 2002, *ApJ*, 577, 311
- Kohri, K., Narayan, R., & Piran, T. 2005, *ApJ*, 629, 341
- Lai, D. 1998, *ApJ*, 502, 721
- Lee, U. 1999, *ApJ*, 511, 359

- Lee, H. K., Wijers, R. A. M. J., & Brown, G. E. 2000, *Phys. Rep.*, 325, 83
- Li, L. X., & Paczynski, B. 2000, *ApJ*, 534, L197
- Li, L. X. 2002, *ApJ*, 567, 463
- Liu, T., Gu, W. M., Xue, L., & Lu, J. F. 2007, *ApJ*, 661, 1025
- Ma, R. Y., Yuan, F., & Wang, D. X. 2007, *ApJ*, 671, 1981
- MacDonald, D., & Thorne, K. S. 1982, *MNRAS*, 198, 345
- McKinney, J. C. 2005, *ApJ*, 630, L5
- Mizuno Y. et al. 2004, *ApJ*, 606, 395
- Narayan, R., Piran, T., & Kumar, P. 2001, *ApJ*, 557, 949 (NPK01)
- Novikov, I. D., & Thorne, K. S. 1973, in *Black Holes, Les Astres Occlus*, ed. B. & C. Dewitt (New York: Gordon & Breach), 343
- Perez-Ramirez, D., de Ugarte Postigo, A., & Gorosabel, J., et al. 2008, arXiv:0810.2107
- Popham, R., & Narayan, R. 1995, *ApJ*, 442, 337
- Popham, R., Woosley, S. E., & Fryer, C. 1999, *ApJ*, 518, 356 (PWF99)
- Pudritz, R. E., & Fahlman, G. G. 1982, *MNRAS*, 198, 689
- Qian, Y. Z., & Woosley, S. E. 1996, *ApJ*, 471, 331
- Reynoso, M. M., Romero, G. E., & Sampayo, O. A. 2006, *A&A*, 454, 11
- Riffert, H., & Herold, H. 1995, *ApJ*, 450, 508
- Rosswog, S., Ramirez-Ruiz, E., & Davies, M. 2003, *MNRAS*, 345, 1077

Sharkura, N. I., & Sunyaev, R. A. 1973, *A&A*, 24, 337

Shibata M. et al., 2006, *PRL*, 96, 031102

Shibata, M., Sekiguchi, Y., & Takahashi, R. 2007, *Progress of Theoretical Physics*, 118, 257

van Putten, M. H. P. M. 1999, *Science*, 284, 115

Wang, D. X., Xiao, K., & Lei, W. H. 2002, *MNRAS*, 335, 655

Wang, D. X., Lei, W. H., & Ma, R. Y. 2003, *MNRAS*, 342, 851

Xie, Y., Huang, C. Y., & Lei, W. H. 2007, *ChJAA*, 7, 685

Ye, Y. C., Wang, D. X., & Ma, R. Y. 2007, *New A*, 12, 471

Zhang B., Fan Y. Z., Dyks J. et al., 2006, *ApJ*, 642, 354

Zhang, D., & Dai, Z. G. 2007, *ApJ*, 683, 329

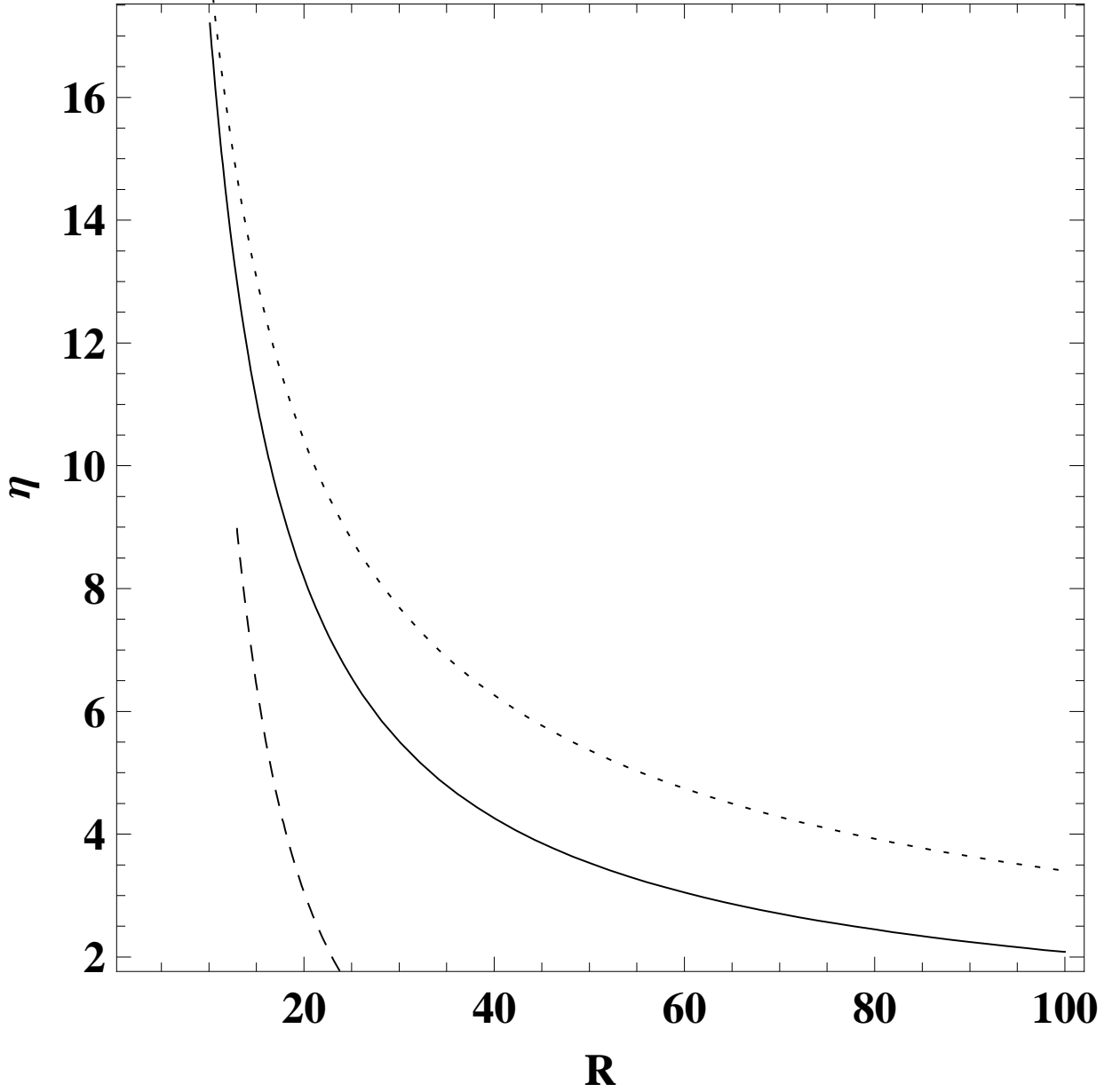


Fig. 1.— The curves of the ratio of Q_{MC} to Q_G versus the disk radius R for $a_* = 0.9$ with $n = 3$ (solid line), $a_* = 0.9$ with $n = 4$ (dotted line) and $a_* = 0.8$ with $n = 3$ (dashed line).

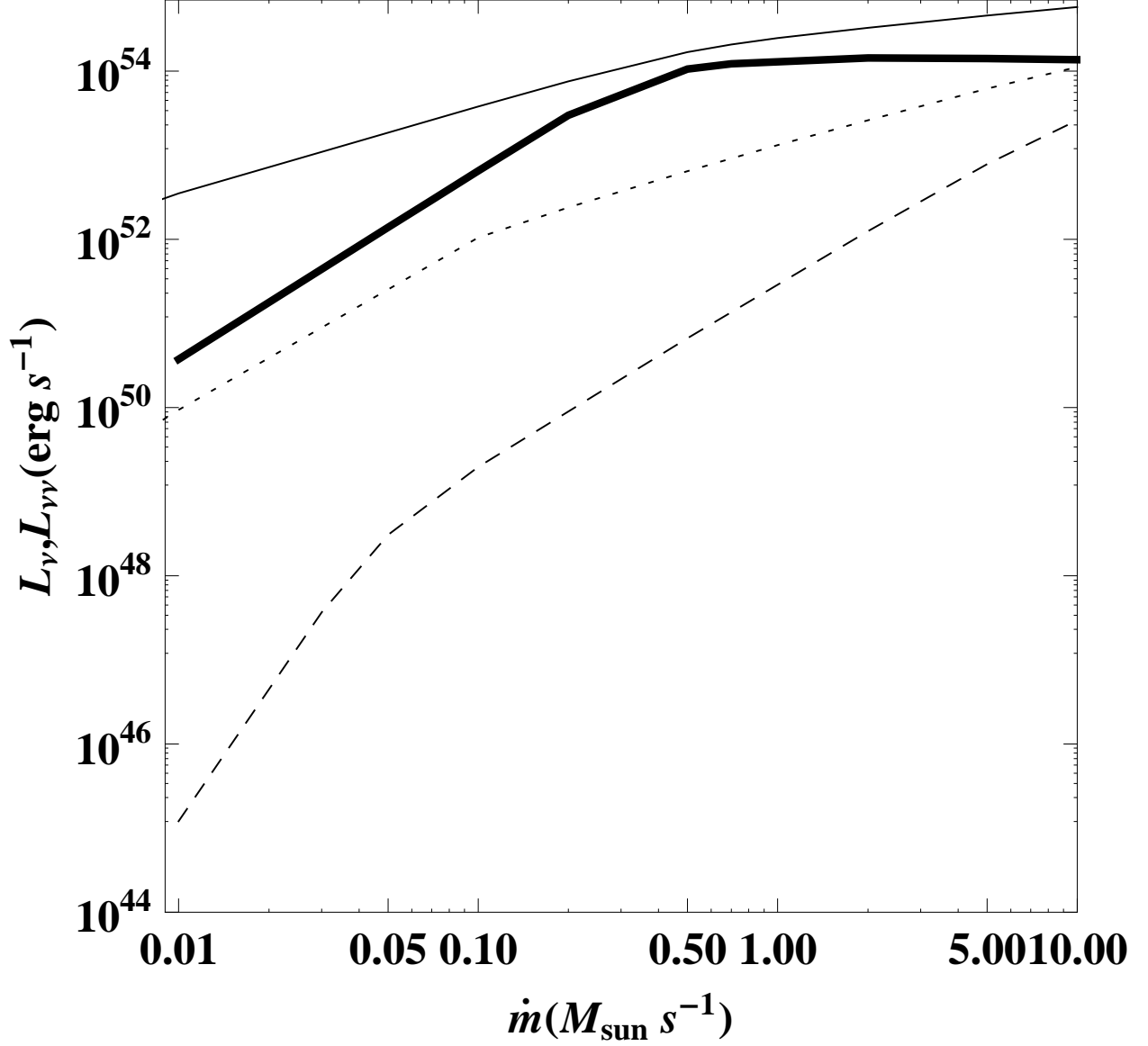


Fig. 2.— The total neutrino luminosity L_{ν} and $L_{\nu\bar{\nu}}$ for $a_* = 0.9$ and $n = 3$. The thick and thin solid lines represent $L_{\nu\bar{\nu}}$ and L_{ν} of MCNDAF, respectively. The dashed line and dotted line represent $L_{\nu\bar{\nu}}$ and L_{ν} of NDAF without MC, respectively.

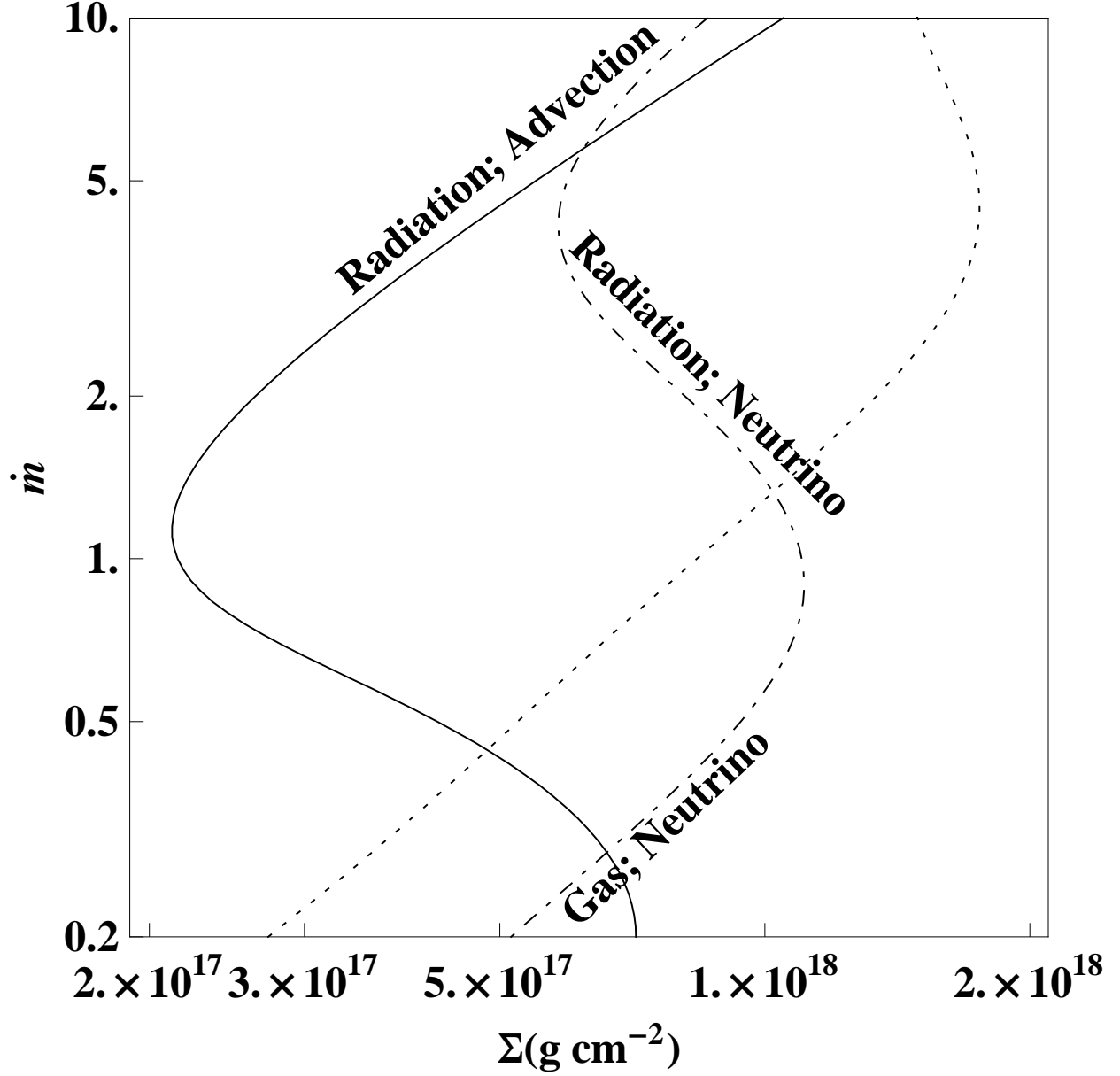


Fig. 3.— The curves of \dot{m} versus Σ for several given disk radii with $R = 5, 10$ and 20 in solid, dashed and dotted lines, respectively. Other parameters are $a_* = 0.9$ and $n = 3$.

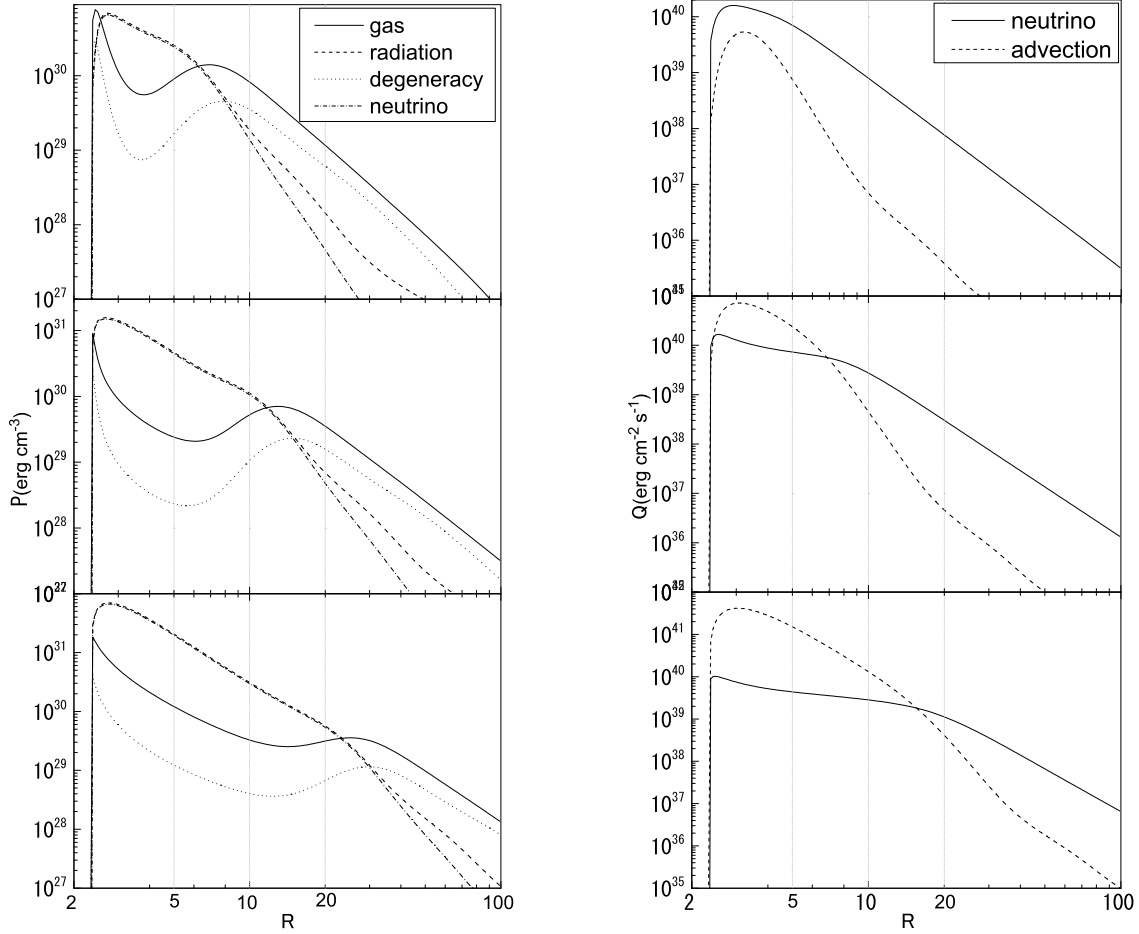


Fig. 4.— Pressure (left) and cooling rate (right) components as a function of the disk radius, for three accretion rate values: $\dot{m} = 0.5$ (top), $\dot{m} = 2$ (middle) and $\dot{m} = 10$ (bottom). The pressure components are: gas pressure (solid line), radiation pressure (dashed line), degeneracy pressure (dotted line), and neutrino pressure (dot-dashed line). The cooling terms are: cooling rates due to neutrino emission (solid line) and advection (dashed line). Other parameters are $a_* = 0.9$ and $n = 3$.

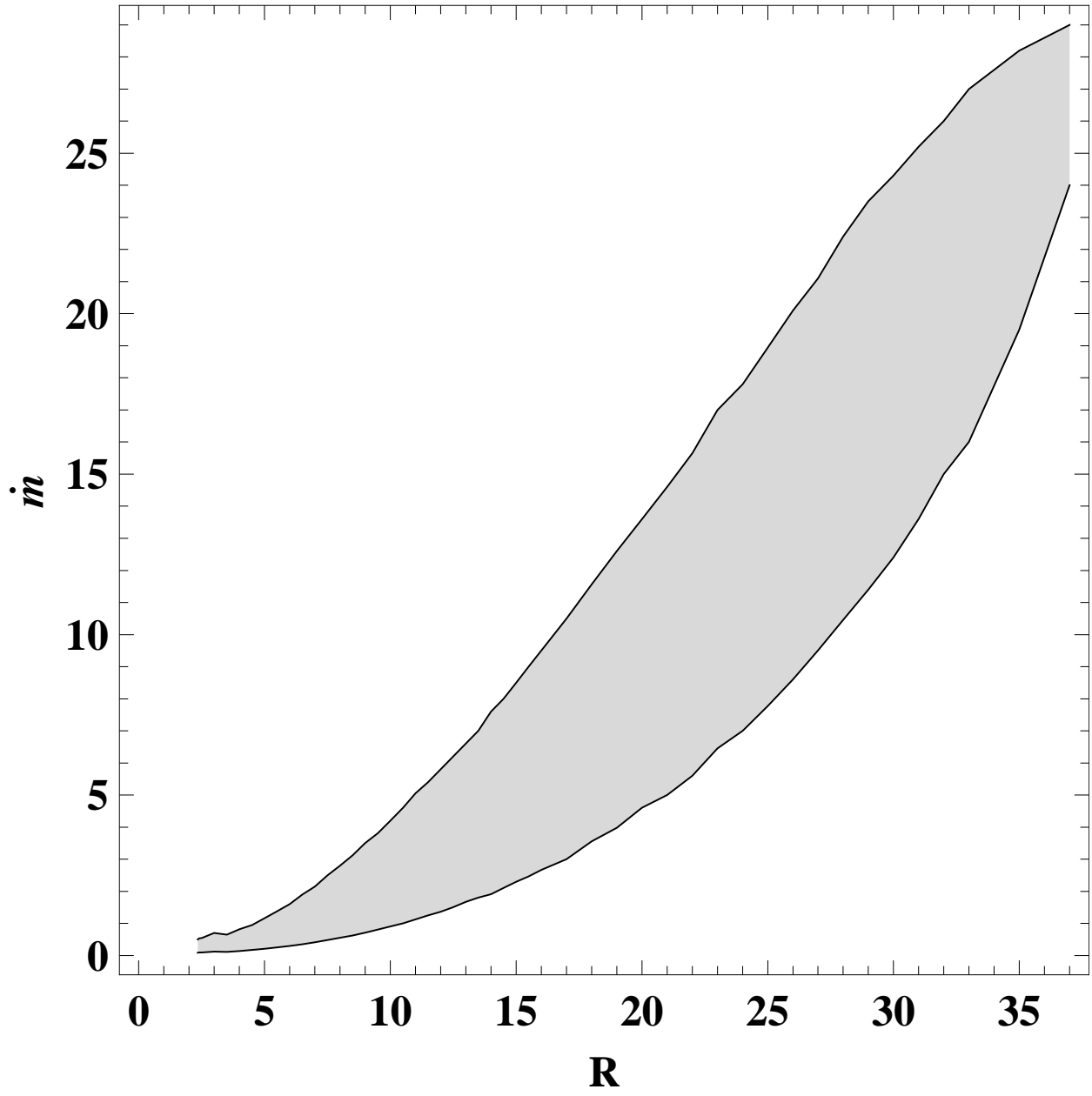


Fig. 5.— The viscous instability is indicated by the shaded region in the parameter space. The parameters are $a_* = 0.9$ and $n = 3$.